*Acc. Chem. Res.* **2006,** *39,* 788−796

# Structural and Electron Paramagnetic Resonance (EPR) Studies of Mononuclear Molybdenum Enzymes from Sulfate-Reducing Bacteria

CARLOS D. BRONDINO,[†] MARÍA G. RIVAS,[‡] MARIA J. ROMÃO,[‡] JOSÉ J. G. MOURA,[‡] AND ISABEL MOURA*,[‡]

*REQUIMTE/CQFB, Departamento de Química, Faculdade de Ciências e Tecnologia, Universidade Nova de Lisboa, 2829-516 Caparica, Portugal, and Facultad de Bioquímica y Ciencias Biológicas, Universidad Nacional del Litoral, 3000 Santa Fe, Argentina*

Received April 20, 2006

**ABSTRACT**

Molybdenum and tungsten are found in biological systems in a mononuclear form in the active site of a diverse group of enzymes that generally catalyze oxygen-atom-transfer reactions. The metal atom (Mo or W) is coordinated to one or two pyranopterin molecules and to a variable number of ligands such as oxygen (oxo, hydroxo, water, serine, aspartic acid), sulfur (cysteines), and selenium (selenocysteines) atoms. In addition, these proteins contain redox cofactors such as iron−sulfur clusters and heme groups. All of these metal cofactors are along an electron-transfer pathway that mediates the electron exchange between substrate and an external electron acceptor (for oxidative reactions) or donor (for reductive reactions). We describe in this Account a combination of structural and electronic paramagnetic resonance studies that were used to reveal distinct aspects of these enzymes.

## Mononuclear Molybdenum Enzymes: Classification and General Properties

Molybdenum and tungsten are found in biological systems in a mononuclear form in the active site of a diverse group of enzymes that generally catalyze oxygen-atom-transfer reactions.[1,2] Mononuclear molybdenum-containing enzymes are ubiquitous and participate in several biological processes occurring in nature, such as denitrification, the greenhouse effect, and pollution of the water soil.[3,4,5]

Mononuclear molybdenum enzymes have been divided into three groups called the xanthine oxidase (XO), dimethyl sulfoxide reductase (DMSOR), and sulfite oxidase (SO) families.[1,6] These three families include not only the enzymes that give the name to the different groups but also diverse enzymes, such as aldehyde oxidoreductases, nitrate reductases, and formate dehydrogenases, among others. The active site of these enzymes (Figure 1a) includes the metal atom coordinated to one or two pyranopterin molecules and to a variable number of ligands such as oxygen (oxo, hydroxo, water, serine, aspartic acid), sulfur (cysteines), and selenium (selenocysteines) atoms. The pyranopterin molecule is an organic ligand that can be either in the monophosphate form or have a nucleotide molecule attached by a pyrophosphate link (Figure 1b).[7] In addition, these proteins may also have other redox cofactors such as iron−sulfur (FeS) centers, hemes, and flavin groups, which are involved in intra- and intermolecular electron-transfer processes. A tungsten-containing aldehyde oxidoreductase from *Pyrococcus furiosus* presents a similar active-site structure and has been classified in a different family.[2] However, other tungsten enzymes such as the formate dehydrogenase from *Desulfovibrio gigas* belong to the DMSOR family, being closely related to the corresponding molybdenum enzymes.[8]

With a few exceptions, these enzymes catalyze the transfer of an oxygen atom from water to the product (or vice versa) in reactions that imply a net exchange of two electrons between the enzyme and substrate and in which the metal ion cycles between the redox states IV and VI. Figure 2 shows two representative examples of half-reactions catalyzed by mononuclear molybdenum enzymes. The members of the XO family catalyze the oxidative hydroxylation of a diverse range of aldehydes (Figure 2a) and aromatic heterocycles in reactions that involve the cleavage of a C−H and the formation of a C−O bond.[9] In contrast, the members of the DMSOR and SO families catalyze the transfer of an oxygen atom to or from a lone electron pair of the substrate (e.g., the reduction of nitrate to nitrite, Figure 2b), with the only exception of the formate dehydrogenases, which catalyze the conversion of formate to $CO_2$ without oxygen incorporation.[8,9] The accepted general mechanism of the reactions catalyzed by these enzymes is shown in Figure 2c. The substrate reacts with the molybdenum center, which is reduced from $Mo^{VI}$ to $Mo^{IV}$ in those reactions that involve the substrate oxidation and oxidized from $Mo^{IV}$ to $Mo^{VI}$ in those reactions occurring in the opposite direction. The two reducing equivalents generated in the course of

* To whom correspondence should be addressed. E-mail: isa@dq.fct.unl.pt. Fax: +351-21-2948550.
[†] Universidad Nacional del Litoral.
[‡] Universidade Nova de Lisboa.

Carlos D. Brondino received his B.S. and Ph.D. degrees from the Universidad Nacional del Litoral (Argentina). He was a postdoctoral and research fellow at the Universidade Nova de Lisboa. He is now a professor and research fellow of CONICET in the Department of Physics of Facultad de Bioquímica y Ciencias Biológicas at the Universidad Nacional del Litoral.

Maria G. Rivas received her B.S. degree from the Universidad Nacional del Litoral (Argentina). She is now a Ph.D. student at the Universidade Nova de Lisboa.

Maria J. Romão received her Ph.D. degree from the Universidade Técnica de Lisboa, and she is now associate professor in the chemistry department of the Universidade Nova de Lisboa, where she is responsible for the group of protein crystallography (http://xtal.dq.fct.unl.pt/).

José J. G. Moura received his Ph.D. degree from the Universidade Nova de Lisboa, and he is now professor of chemistry in the chemistry department of the Universidade Nova de Lisboa, where he is responsible for the group of bioinorganic chemistry and protein engineering.

Isabel Moura received her Ph.D. degree from the Universidade Nova de Lisboa, and she is now professor of biochemistry in the chemistry department of the Universidade Nova de Lisboa, where she is responsible for the group of biophysical chemistry of proteins.



10.1021/ar050104k CCC: $33.50 
Published on Web 08/25/2006

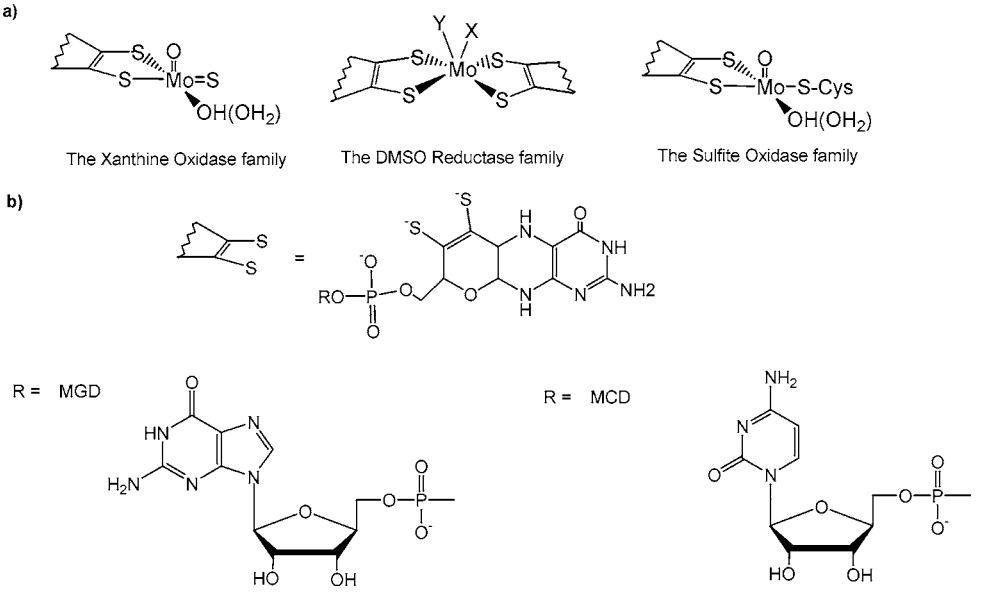


**FIGURE 1.** (a) Active-site structure of the three families of mononuclear molybdenum- and tungsten-containing enzymes. X and Y represent ligands such as oxygen (oxo, hydroxo, water, serine, and aspartic acid), sulfur (cysteine), and selenium (selenocysteine) atoms. (b) Structure of the pyranopterin molecule.

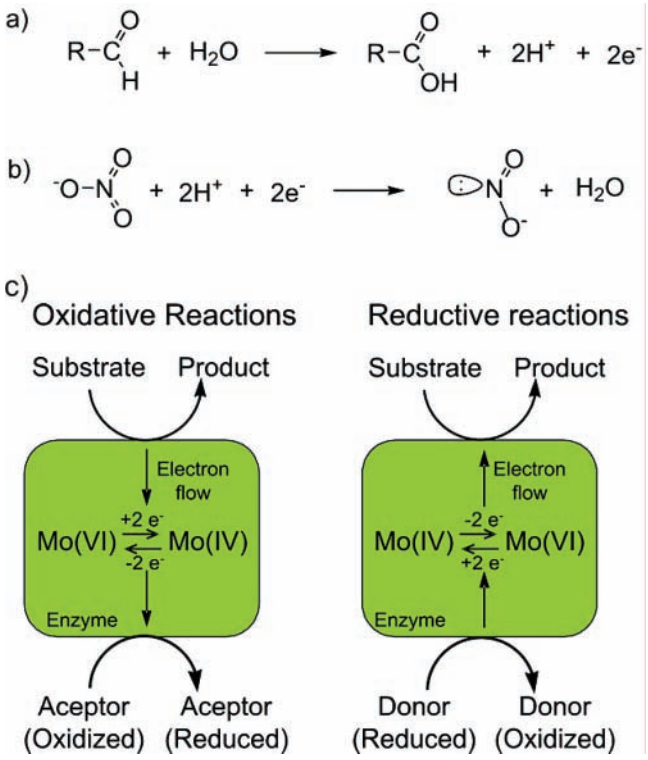


**FIGURE 2.** (a) Half-reaction catalyzed by the enzyme aldehyde oxidoreductase of the XO family. (b) Half-reaction catalyzed by the enzyme nitrate reductase, which, depending upon the source, can belong to either the DMSOR or SO family. (c) Accepted general mechanism for oxidative (left) and reductive (right) reactions catalyzed by mononuclear molybdenum-containing enzymes.

oxidative reactions are then transferred to an external electron acceptor by means of an electron-transfer process mediated by other redox cofactors present in the structure of these proteins. In contrast, two reducing equivalents given by an external electron donor are consumed by the substrate in reductive reactions, and the electron flow occurs in the opposite direction.

Our work in molybdenum-containing enzymes has been centered in the characterization of a number of enzymes obtained from sulfate-reducing bacteria (SRB). SRB constitute a group of microorganisms sharing the ability of using sulfate for their growth, with the production of large amounts of hydrogen sulfide.[10] Aldehyde oxidoreductase (Aor) and Formate dehydrogenase (Fdh) from SRB, which belong to the XO and DMSOR family, respectively, are representative examples of these proteins. Whereas aldehyde oxidoreductases are exclusively molybdenum-containing enzymes, formate dehydrogenases can incorporate either molybdenum or tungsten depending upon the case. We describe in this Account a combination of structural and electronic paramagnetic resonance (EPR) studies that were used to learn about distinct aspects of these two enzymes.

## Molecular Properties and Overall Folding of Aldehyde Oxidoreductases and Formate Dehydrogenases from SRB

Aldehyde oxidoreductases from the SRB *Desulfovibrio gigas* (*Dg*),[11] *Desulfovibrio desulfuricans* (*Dd*),[12] *Desulfovibrio alaskensis* (*Da*),[13] and *Desulfovibrio aminophilus* (*Dam*)[14] are homodimeric proteins (~100 kDa per monomer) that contain molybdenum at the active site. The structures of *Dg* Aor, the first structure reported for a mononuclear molybdenum-containing enzyme,[15,16] and *Dd* Aor[17] were solved at the resolution of 1.28 and 2.8 Å, respectively. The 3D structure of each monomer is organized into two major domains called Mo and FeS domains (Figure 3a). The Mo domain is the largest one and contains the active site, whereas the FeS domain contains two [2Fe−2S] centers called FeS I and II. The [2Fe−2S]

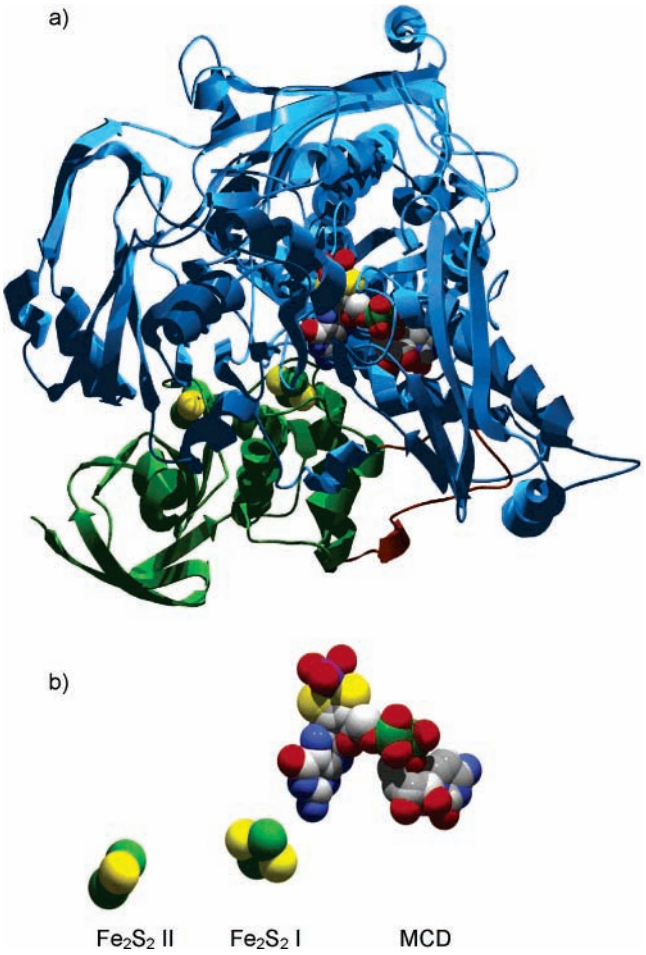


**FIGURE 3.** (a) Overall structure of the molybdenum-containing enzyme *Dg* Aor. (b) Arrangement of the redox cofactors involved in electron transfer.

centers are iron dimers (Fe−Fe distances ∼ 2.7 Å), in which the Fe ions are coordinated by two bridging sulfido ligands and by two cysteine thiolates (Figure 3b). Other members of the XO family have in addition a third domain (the FAD domain) that contains a flavin cofactor. The crystal structures of some of these proteins are compared in ref 18.

Formate dehydrogenases from three SRB have been isolated and characterized. *Dg* Fdh[19] and *Da* Fdh[20] are heterodimers, whereas *Dd* Fdh is a heterotrimer.[21] The α subunit (∼90 kDa) of these proteins includes the active site and one [4Fe−4S] center, whereas the $\beta$ subunit (∼29 kDa) contains three additional [4Fe−4S] centers. The [4Fe−4S] clusters have a cubane-type structure with Fe−Fe distances similar to those of the [2Fe−2S] clusters, in which sulfido ligands bridge three Fe ions and each Fe iron is coordinated by one cysteine thiolate. *Dd* Fdh has a third subunit (∼16 kDa), which was suggested to contain four *c*-type hemes.[21] In contrast to aldehyde oxidoreductases that only incorporate molybdenum, formate dehydrogenases from SRB have been detected with different metal ions (Mo or W) at the active site. This characteristic was also observed in other formate dehydrogenases belonging to the DMSOR family, which mostly incorporate molybdenum, but a number of them can incorporate

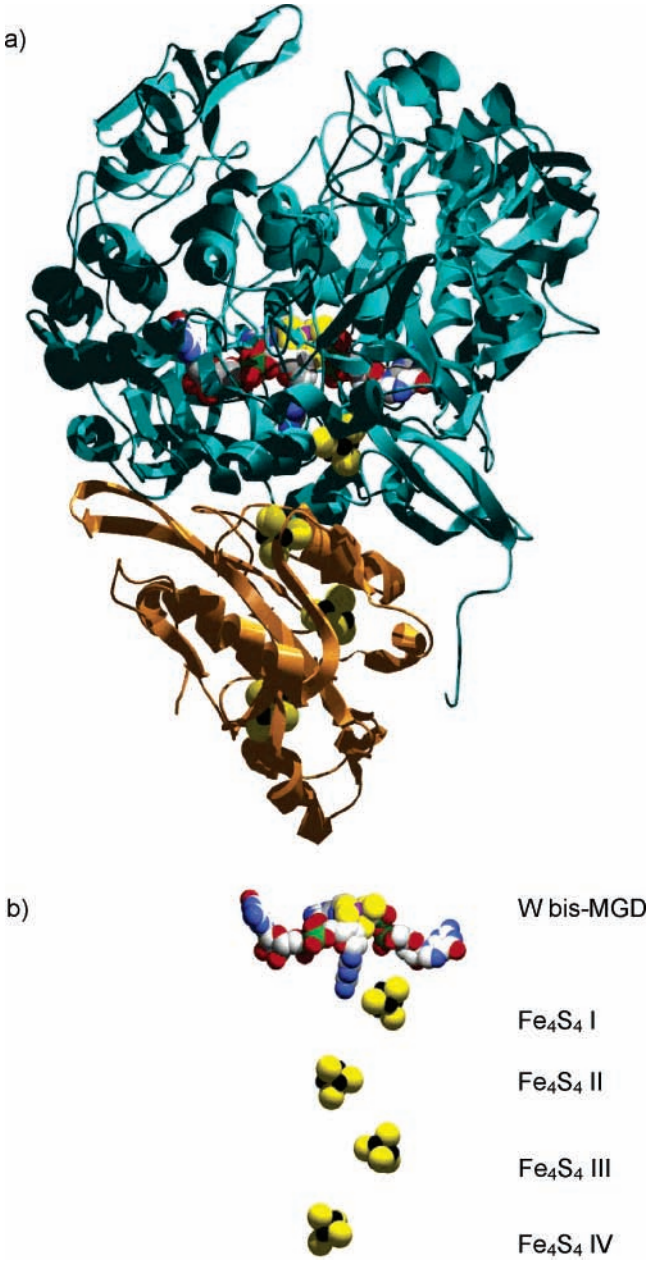


**FIGURE 4.** (a) Overall structure of the tungsten-containing enzyme *Dg* Fdh. (b) Arrangement of the redox cofactors involved in electron transfer.

tungsten.[8] Despite the fact that tungsten and molybdenum exhibit analogous chemical properties, the reasons for the incorporation of either molybdenum or tungsten in enzymes is far from being elucidated and these can, apparently, be divided into redox properties of the enzyme, bioavailability of the metal ions, and evolution.[8,22]

The only crystal structure reported for a Fdh from SRB is the tungsten-containing *Dg* Fdh.[23,24] The tungsten-containing enzyme *Dg* Fdh is a heterodimeric enzyme with 92 and 29 kDa subunits, respectively (Figure 4). The large subunit can be divided in four domains (I, II, III, and IV). The tungsten active site is buried inside the protein and is stabilized by hydrogen-bonding interactions to residues of mainly domains II, III, and IV. Domain I carries the characteristic cysteine motif that binds the first

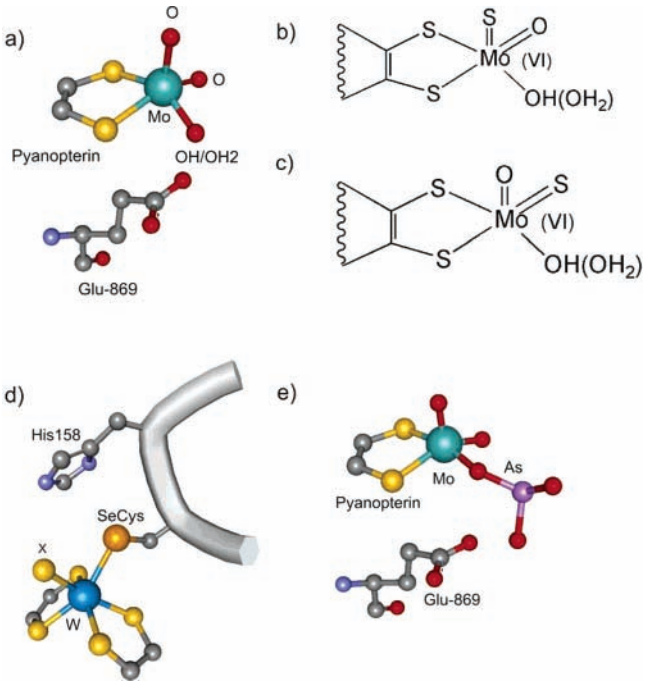


**FIGURE 5.** (a) Coordination around molybdenum in *Dg* AOR. The side chain of a glutamate residue, conserved in all of the members of the XO family, is also included. (b and c) Coordination around molybdenum in the XO family with two different coordination modes of the sulfido ligand: (b) as found in the crystal structure of *Dg* AOR resulfurated crystals[25] and (c) as found in the crystal structure of QOR[26] and BXDH.[27] (d) Coordination around the tungsten atom in oxidized *Dg* Fdh. Ligand X was proposed to be a sulfur atom in *Dg* Fdh and an oxygen atom in the closely related *Ec* Fdh-H and *Ec* Fdh-N. (e) Geometry of the arsenite-inhibited catalytic center in *Dg* AOR.

[4Fe−4S] center (−CXXCX$_n$CX$_m$C−). The N terminus of the large subunit wraps around the smaller subunit and contributes to the stability of the functional heterodimer. The small subunit is of the $\alpha\beta$ type and contains three domains identified as A, B, and C. Domain A holds two iron−sulfur clusters, and domain B holds one center. The fold of domains A and B is similar to 2× [4Fe−4S] ferredoxins. *Dg* Fdh is closely related to the molybdenum-containing Fdh-H and Fdh-N from *Escherichia coli*. A detailed comparison of the crystal structures of these three proteins was reported in ref 8.

## Active-Site Structures: Detecting the Position of the Essential Ligands in Catalysis

The crystal structure of *Dg* Aor showed that the active site consists, in the Mo$^{VI}$ state, of a molybdenum atom in a square pyramidal geometry coordinated by two sulfur atoms from one pyranopterin ligand, two oxo ligands, and one hydroxyl/water molecule (Figure 5a).[15,16] However, studies in aldehyde oxidoreductases and other members of the XO family detected the presence of a sulfido ligand coordinated to molybdenum, which was shown to be essential for catalysis.[1] This suggests that in *Dg* Aor the crystallization selects only the desulfo form of the enzyme. Alternatively, the sulfido ligand may be lost during crystallization to give a desulfo form of the enzyme.

To elucidate the position of the sulfido ligand, "resulfurated" *Dg* AOR single crystals were prepared by soaking with a large excess of sulfide ions. These experiments showed that a sulfido ligand is coordinated in the apical position (Figure 5b).[25] In contrast, the X-ray structure of two other closely related proteins, quinoline 2-oxidoreductase from *Pseudomonas putida* 86[26] and bovine milk xanthine dehydrogenase (BXDH),[27] the latter determined with a substrate analogue bound to the molybdenum atom, showed that the sulfido ligand is at the position of the equatorial oxo group (Figure 5c). The high homology observed between most members of the XO family suggests that the presence of the sulfido ligand in an apical position in *Dg* AOR is either a product of the resulfuration conditions or a distinctive feature of aldehyde oxidoreductases from SRB.

The second essential ligand in catalysis is the equatorial hydroxyl/water ligand. Pioneer works in the XO family member BXDH identified that an oxygen ligand bound to molybdenum is incorporated into the substrate in the course of the catalytic reaction.[28] This catalytic-labile site, which is, after being transferred, reformed from the solvent, was initially thought to be an oxo group, and later, with the report of the structure of *Dg* AOR,[15] it was proposed to be the hydroxyl/water ligand coordinated to molybdenum in an equatorial position (Figure 5a). This was recently confirmed with the crystal structure of a substrate-bound form of BXDH that shows that the substrate molecule binds the enzyme through this ligand.[27]

The coordination around tungsten in oxidized *Dg* Fdh is distorted hexacoordinated (Figure 5d). The sulfur atoms are provided by the dithiolene side chain of two pterin ligands, which have attached a guanine dinucleotide. The metal site is also coordinated to a secysteine residue, which is highly conserved in formate dehydrogenases that belong to the DMSOR family and is supposed to have an essential role in the catalytic mechanism. Finally, the sixth coordination position is occupied by a ligand named X in Figure 5d. Similar coordination geometries were observed in the closely related Fdh-H[29] and Fdh-N[30] from *E. coli*. Ligand X was identified as an oxygen in the X-ray structure of *Ec* Fdh-N (1.6 Å resolution) and *Ec* Fdh-H (2.8 Å resolution) and from EXAFS data in *Ec* Fdh-H[31] and *Dd* Fdh.[32] In contrast, X-ray data in the tungsten-containing *Dg* Fdh (1.8 Å resolution) point to a sulfur atom for this position.[23,24]

Less information exist on the essential ligands for catalysis in formate dehydrogenases because of the lack of structural data of both substrate- and inhibitor-bound forms of these enzymes. On the basis of structural and spectroscopic data in *Ec* Fdh-H,[29,33] it is supposed that the substrate binds the enzyme in the position of ligand X, which, after enzyme−substrate interaction, moves away. However, the detection of a sulfido ligand in this position for the tungsten-containing *Dg* Fdh suggests that this process is unlikely because of the inherent complication of binding a sulfido ligand to molybdenum after product release. Additional work is necessary to confirm whether this sulfido ligand is a particular characteristic of the

tungsten-containing formate dehydrogenases and, in such a case, its implications in catalysis.

## EPR Characterization of the Metal Centers

Because the metal centers of these proteins are paramagnetic in some redox states, EPR has been a valuable tool in their characterization. The molybdenum (tungsten) ion of the active site can be found in three different redox states, $Mo^{VI}$, $Mo^{V}$, and $Mo^{IV}$. Of all of these redox states, $Mo^{V}$ and $W^{V}$ ($S = {}^1/_2$) yield usually EPR signals with all $g$ values lower than 2. The $W^{V}$ ions give signals with larger deviations from the free-electron $g$ value (2.0023) and larger line widths compared to the signals associated with $Mo^{V}$ species. $Mo^{V}$ and $W^{V}$ may also give signals with one of the $g$ values above 2, which are usually associated with those cases where the metal ion is coordinated to a selenocysteine or cysteine ligand. Furthermore, it has been suggested that molybdenum can be also present in the redox state $Mo^{III}$. Although this redox state has been detected and characterized by EPR in some inorganic complexes,[34] there is no strong evidence supporting the presence of this redox state in mononuclear molybdenum enzymes.

The different FeS centers can be obtained in different redox states, with some of them being paramagnetic. The [2Fe−2S] centers can be detected in two redox states, in which the two Fe ions are antiferromagnetically coupled. The oxidized state of this cluster ($[2Fe-2S]^{2+}$) contains two $Fe^{3+}$ ions with a ground state with $S = 0$, which is diamagnetic but becomes a cluster with $S = {}^1/_2$ upon reduction because one of the $Fe^{3+}$ ions is reduced to $Fe^{2+}$. In contrast, the [4Fe−4S] clusters can be obtained in at least three different redox states, with the most common being the states $[4Fe-4S]^{+2}$ and $[4Fe-4S]^{+1}$. The configuration $[4Fe-4S]^{+2}$ comprises 2× $Fe^{2+}$ and 2× $Fe^{3+}$ with a ground state with $S = 0$, which is diamagnetic and cannot be detected by EPR, but, in contrast, the configuration $[4Fe-4S]^{+1}$ is composed of 3× $Fe^{2+}$ and 1× $Fe^{3+}$, which in all of the cases analyzed here gives a paramagnetic ground state with $S = {}^1/_2$.

The FeS centers in aldehyde oxidoreductases and formate dehydrogenases from SRB can be identified from their different redox properties, EPR parameters, and relaxation behaviors. These centers have redox potentials below −200 mV and can be completely transformed to their paramagnetic forms using dithionite as a reductant. We show in Figure 6 EPR data obtained in the dithionite reduced state of *Da* Fdh, in which one can see the different EPR signals associated with the four different FeS clusters present in the structure of formate dehydrogenases from SRB (Figure 4). The fast relaxation properties of these centers determine that their EPR spectra are detected at temperatures below 100 K. The spectrum of Figure 6a (FeS I, $g_1 = 1.882$, $g_2 = 1.946$, and $g_3 = 2.046$) appears at temperatures below 70 K and shows no significant broadening below 40 K. A second broader rhombic EPR signal (FeS II, $g_1 = 1.868$, $g_2 = 1.913$, and $g_3 = 2.066$) overlapped to that of FeS I appears around 25 K

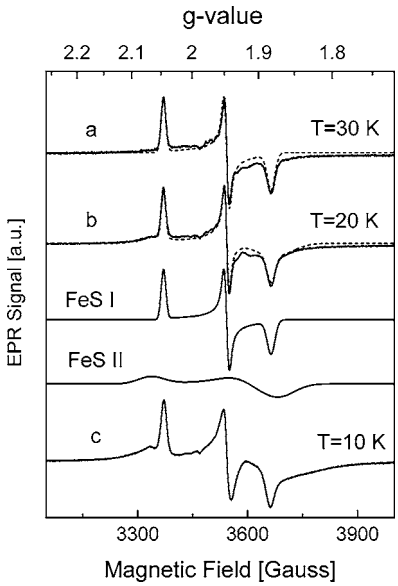


**FIGURE 6.** Variable-temperature EPR spectra (a−c) taken in the dithionite-reduced state of *Da* Fdh. The signals FeS I and II and dashed lines are simulations. The EPR parameters used in the spectral simulation were $g_1 = 1.882$, $g_2 = 1.946$, and $g_3 = 2.046$ for FeS I and $g_1 = 1.868$, $g_2 = 1.913$, and $g_3 = 2.066$ for FeS II (see ref 20 for details).

(Figure 6b). The spectra below 15 K (Figure 6c) show additional broad features overlapped to the signals of centers FeS I and II, which arise from the remaining FeS centers (FeS III and IV).

## Assignment of the EPR Active Centers with Those Seen in the Crystal Structure

An usual problem in studying metalloproteins is to assign the metal centers detected by spectroscopy with those observed in the X-ray structure. We have solved this problem using two different strategies, which are both based in the analysis of the weak magnetic interactions between the redox cofactors. Weak magnetic couplings between interacting centers may be produced by spin−spin interactions such as dipolar and isotropic, antisymmetric, and anisotropic exchange.[35] Dipolar couplings and anisotropic and antisymmetric exchange may produce anisotropic splittings of the resonance lines, whereas, in contrast, isotropic exchange interactions between two anisotropic paramagnets predict an isotropic splitting with a magnitude of $J(H_{ex} = J\mathbf{S}_1\mathbf{S}_2)$ when $|J| < |\Delta g \beta B|$, where $\Delta g$ is the difference between the effective $g$ values of both centers, $\beta$ is the Bohr magneton, and $B$ is the external magnetic field. Furthermore, if one of the species of the interacting pair had a relaxation rate ($T_1$) faster than the other one, it would produce an enhancement of the relaxation rate of the slow-relaxing paramagnetic center, leading to a temperature dependence of the splitting produced by the magnetic couplings.[36] This effect is produced because of the dependence of the relaxation time $T_1$ with temperature: the shorter the $T_1$ of the fast-relaxing center (or, equivalently, the higher the temperature), the higher the enhancement of relaxation prop-

erties of the slow-relaxing center. Examples of temperature-dependent magnetic interactions have been observed in all aldehyde oxidoreductases from SRB and in *Da* Fdh, in which the $Mo^V$ ion of the active site is coupled to the closest FeS center.[20,37]

One of the strategies to correlate EPR with crystal data can be used when the redox potential of the interacting centers with $Mo^V$ ions are different, even when this difference is as small as 50 mV, as is the case for *Da* Aor.[13] *Da* Aor (and all aldehyde oxidoreductases from SRB) shows two EPR signals named FeS I ($g_1 = 1.916$, $g_2 = 1.934$, and $g_3 = 2.021$) and FeS II ($g_1 = 1.900$, $g_2 = 1.970$, and $g_3 = 2.066$), which are associated with the two [2Fe−2S] clusters detected from X-ray data in aldehyde reductases (Figure 3). The methodology, which should be the elected one for simplicity, consists of poising the redox potential of the enzyme solution to a potential at which the FeS centers are not completely reduced, and at least a fraction of the molybdenum is present as $Mo^V$ (midpoint redox potentials for FeS I and II are −275 and −325 mV, respectively). Figure 7a shows the different microstates that can be obtained at different levels of reduction of *Da* Aor, whereas Figure 7b shows the EPR spectra obtained at 20 K and at the potentials −450 and −334 mV. At −450 mV, the FeS centers are completely in the paramagnetic redox state with $S = {}^1/_2$, and hence, all of the $Mo^V$ ions are magnetically coupled to the closest FeS center. The splitting of FeS I at $g_{max}$ is due to the interaction between FeS I and II. This situation corresponds to the microstates $P_{10} + P_7 + P_{11}$, in which both $Mo^V$ and FeS I signals are fully split. In contrast, the spectrum at −325 mV results from the superposition of both split ($P_5 + P_{10}$) and nonsplit components ($P_1 + P_6$) for the $Mo^V$ signal. A similar reasoning can be used to interpret the resulting signal for the FeS I center. Using the midpoint redox potential of each center at such a potential, it is possible to predict the proportion of each component contributing to the EPR signal as a function of the potential. The simulations in Figure 7b were obtained assuming that FeS I (sim-a) and FeS II (sim-b) are, respectively, the center closer to molybdenum. A good agreement between simulation and experiment was obtained for sim-a, confirming that the center giving the FeS I signal is the cluster proximal to the molybdenum.

The second strategy must be used in those cases in which the EPR signals cannot be discriminated with a redox titration or when the amount of protein samples is not enough to perform the experiment described before. Figure 8 shows the variation with temperature of the $Mo^V$ signal in *Da* Fdh. At temperatures above 100 K, the spectra show an almost axial symmetry ($g_1 = 1.959$, $g_2 = 1.968$, and $g_3 = 1.971$) with resonances split by a single proton ($A_1 = 14$ G, $A_2 = 16$ G, and $A_3 = 16$ G). As the temperature is decreased, this signal is first broadened and then fully split at temperatures lower than 50 K (no changes can be observed above 100 K and below 50 K). Furthermore, the splitting of the $Mo^V$ signal at low temperatures is isotropic, which indicates that, as discussed above, the isotropic

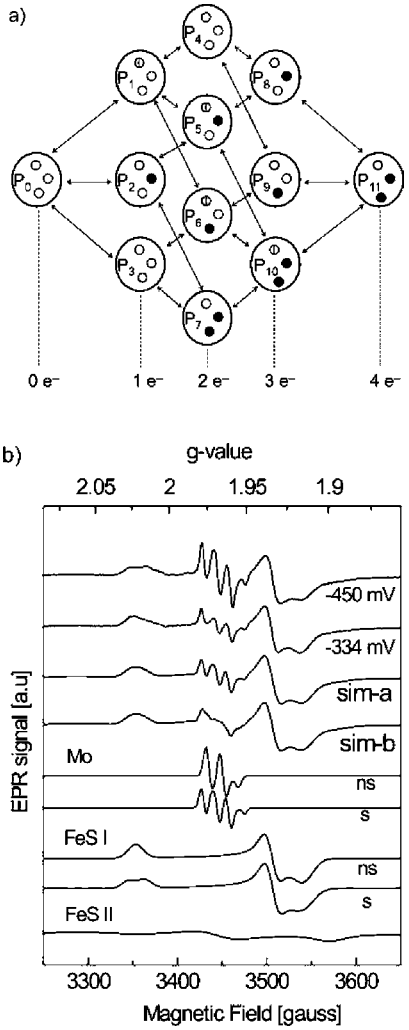


**FIGURE 7.** (a) Schematic representation of the 12 possible microstates in *Da* Aor molecules at different levels of reduction. The upper circle represents the molybdenum atom, and the middle and lower circles represent any of the FeS centers. The open circle represents oxidized FeS or $Mo^{VI}$; the half-open/half-closed circle represents $Mo^V$, and the closed circle represents reduced FeS centers or $Mo^{IV}$. The double-headed arrows connect microstates separated by one-electron reduction/oxidation ($P_0$ and $P_{11}$ represent the fully oxidized and reduced states, respectively) (b) EPR spectrum of *Da* Aor samples at −450 and −334 mV. Simulation sim-a was obtained considering that FeS I is the center closer to Mo, whereas sim-b was obtained considering that FeS II is the closer one. The symbols "s" and "ns" stand for split and nonsplit signals, respectively.

exchange interaction is the main interaction operating between the coupled centers.

The temperature dependence of the $Mo^V$ ion spectra shown in Figure 8A was simulated assuming a dimeric model composed of two interacting $S = {}^1/_2$ centers relaxing independently, including in addition the hyperfine coupling with a nucleus of nuclear spin $I = {}^1/_2$ at one of the centers, with both centers being magnetically coupled only by the isotropic exchange interaction.[38] The results of this simulation as a function of the relaxation time $T_1$ of the faster relaxing center is shown in Figure 8B. Details of the model employed in the simulation are given in ref 20, and the dependence with temperature of

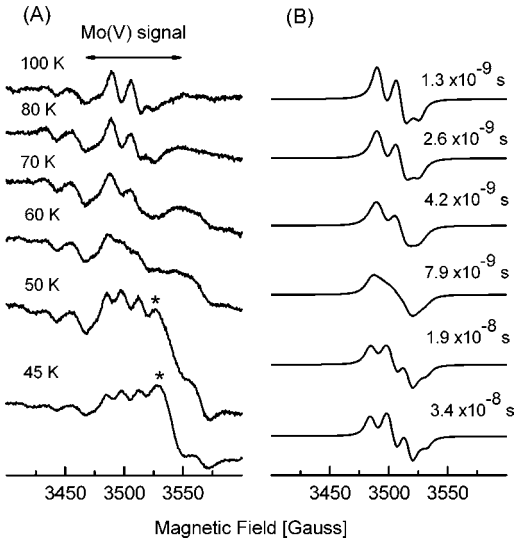


**FIGURE 8.** Temperature variation of the EPR signal associated with $Mo^V$ ions in *Da* Fdh (A) and spectral simulation as a function of the relaxation time ($T_1$) of FeS I (B) (see ref 20 for details). The peaks marked with an asterisk originate from overlapping signals associated with the $g_{med}$ feature of the FeS I center (see Figure 6) and that of the $g_{max}$ of the $W^V$ signal (not shown).

the $T_1$ values was evaluated following methods described in ref 39. The results showed a good matching between experiment and simulation using the relaxation time $T_1$ associated with FeS I. This indicates that the center named FeS I in the EPR experiment is the center that interacts magnetically with the molybdenum center and therefore is situated in the α subunit of the protein. Similar ideas were used to assign the proximal FeS center in the proteins of the XO family *Dg* Aor and BXDH but with a model based on the semiempirical Bloch equations.[37]

## Evaluating the Characteristics of the Active Site and Electron-Transfer Pathways in Inhibited-Enzyme Forms

Inhibitors of the enzymes belonging to the XO family such as arsenite, alcohols, and glycols can react with the molybdenum site, constituting important structural probes for screening the coordination of the active site as well as elucidating the inhibition mechanism. Part of our work in aldehyde oxidoreductases from SRB has been directed to elucidate whether the catalytic-labile site is also the site for enzyme inhibition and how the electron-transfer pathway is modified upon inhibition. EPR experiments on dithionite-reduced arsenite-inhibited *Dg* Aor showed that the arsenic atom interacts with the molybdenum ions through strong hyperfine and quadrupolar interactions.[40] The experiment conducted on $D_2O$-exchanged samples was similar, which led us to suppose that the arsenic atom interacts likely through the equatorial OH/water ligand to molybdenum (Figure 5a). This was confirmed with X-ray data taken on single crystals of *Dg* Aor soaked with a buffer containing $NaAsO_2$. In this structure, the arsenic atom is bound to three oxygen atoms, with one of them in a bridging position between molybdenum and arsenic atoms (Figure 5e). This bridging ligand is in the position of the catalytically labile site, and the $AsO_3$ moiety is positioned so that one of the oxygen atoms is within hydrogen-bonding distance to glutamate 869, a conserved residue essential for catalysis.

The integrity of the electron-transfer pathway upon enzyme inhibition was also investigated. The reaction mechanism involves the substrate binding to the active site followed by two-electron transfer to the partner of the redox reaction in an electron-transfer reaction mediated by the FeS centers. A structural comparison of the arsenite-inhibited form with the as-prepared form of *Dg* Aor showed no significant changes, apart from the differences at the active site. This suggests that the electron-transfer pathway, which is essential for catalysis, is not affected upon inhibition. This was confirmed by means of EPR saturation studies in oxidized and reduced forms of arsenite-inhibited *Dg* Aor. Air oxidation of reduced samples oxidizes the FeS clusters to a diamagnetic state but leaves the molybdenum as $Mo^V$. Thus, we can evaluate the saturation of the $Mo^V$ species in two redox forms of the enzyme, one showing magnetic coupling between molybdenum and FeS I and another one where no magnetic coupling between the centers is observed, which can be advantageously used to evaluate changes in the relaxation properties of the $Mo^V$ ion. These studies showed that the relaxation properties of molybdenum are enhanced in the reduced samples, which indicates that the chemical pathway connecting molybdenum and FeS I can transmit a magnetic interaction in the inhibited form of the enzyme. This study confirmed that the postulated electron-transfer pathway is not affected and that the enzyme inhibition occurs only by blocking the catalytic-labile site.

## Concluding Remarks and Perspectives

After 4 decades of hard investigation on mononuclear molybdenum proteins, several points remains enigmatic.[41] The crystal structures of various members of these enzymes have undoubtedly contributed to a better understanding of these proteins. In addition, spectroscopic data have been a valuable tool to understand fine details of the structure that cannot be solved with X-ray data. One of the major problems of these investigations is the lack of structural data obtained at different redox states of the proteins. In several cases, this has prevented one from establishing clear correlations between spectroscopic and structural data because they must be interpreted in terms of the structural data of the oxidized enzyme. To solve this problem, we have implemented a methodology that consists of measuring the EPR properties of frozen polycrystalline samples, which are then used for X-ray experiments. This method is, in principle, applicable to any system containing a paramagnetic center and suitable for single-crystal X-ray diffraction analysis. The success of the method depends upon the possibility for diffusion of reactants into the crystals and whether the crystals remain suitable for diffraction analysis after repeated thawing and freezing and after exposure to the reactant(s) (e.g., dithion-

ite). This method has been recently utilized to assign the EPR signals of arsenite-inhibited samples of *Dg* Aor to the molecular structure of the molybdenum site (Thapper, A.; Boer, D. R.; Brondino, C. D.; Moura, J. J. G.; Romão, M. J. 2006, manuscript submitted) and is currently tested for other mononuclear molybdenum enzymes. We believe that the application of new methodologies together with new structural and spectroscopic studies on a larger number of proteins can contribute to a better understanding of the molecular processes that occur during catalysis. This constitutes one of the most important challenges for the next few years.

*This work was supported by projects EC HPRN-CT-1999-00084, POCTI/1999/BME/35078, POCTI/1999/BME/36152, and POCTI/QUI/57641/2004 in Portugal and SEPCYT:PICT 2003-06-13872, CONICET PIP 53709/2005, and CAI+D-UNL in Argentina. M. G. R. thanks Fundação para a Ciência e a Tecnologia for a fellowship grant (SRFH/BD/10784/2002). C. D. B. and J. J. G. M. thank SECYT (Argentina) and GRICES (Portugal) for a binational grant. C. D. B. is a member of CONICET.*

## References

(1) Hille, R. The mononuclear molybdenum enzymes. *Chem. Rev.* **1996**, *96*, 2757−2816.
(2) Johnson, M. K.; Rees D. C.; Adams, M. W. Tungstoenzymes. *Chem. Rev.* **1996**, *96*, 2817−2840.
(3) Moriwaki, Y.; Yamamoto, T.; Higashino, K. Distribution and pathophysiologic role of molybdenum-containing enzymes. *Histol. Histopathol.* **1997**, *12*, 513−524.
(4) Zumft, W. G. Cell biology and molecular basis of denitrification. *Microbiol. Mol. Biol. Rev.* **1997**, *61*, 533−616.
(5) Hamilton, W. A. Microbially influenced corrosion as a model system for the study of metal microbe interactions: A unifying electron-transfer hypothesis. *Biofouling* **2003**, *19*, 65−76.
(6) Romão, M. J.; Knablein, J.; Huber, R.; Moura, J. J. Structure and function of molybdopterin containing enzymes. *Prog. Biophys. Mol. Biol.* **1997**, *68*, 121−144.
(7) Romão, M. J.; Huber, R. Structure and function of the xanthine-oxidase family of molybdenum enzymes. In *Metal Sites in Proteins and Models—Redox Centers, Structure and Bonding*; Hill, H. O. A., Sadler, P. J., Thomson, A. J., Eds.; Springer-Verlag: Berlin, Germany, 1998; Vol. 90, pp 69−96.
(8) Moura, J. J.; Brondino C. D.; Trincao, J.; Romão, M. J. Mo and W bis-MGD enzymes: Nitrate reductases and formate dehydrogenases. *J. Biol. Inorg. Chem.* **2004**, *9*, 791−799.
(9) Romão, M. J.; Cunha, C. A.; Brondino, C. D.; Moura, J. J. *Met. Ions Biol. Syst.* **2002**, *39*, 539−570.
(10) Widdel, F. Microbiology and ecology of sulfate- and sulfur-reducing bacteria. In *Biology of Anaerobic Microorganims*; Zehnder, A. J. B., Ed.; John Wiley and Sons: New York, 1988; pp 469−585.
(11) Moura, J. J. G.; Xavier, A. V.; Bruschi, M.; Le Gall, J.; Hall, D. O.; Cammack, R. A molybdenum-containing iron−sulphur protein from *Desulphovibrio gigas. Biochem. Biophys. Res. Commun.* **1976**, *72*, 782−789.
(12) Duarte, R. O.; Archer, M.; Dias, J. M.; Bursakov, S.; Huber, R.; Moura, I.; Romão, M. J.; Moura, J. J. Biochemical/spectroscopic characterization and preliminary X-ray analysis of a new aldehyde oxidoreductase isolated from *Desulfovibrio desulfuricans* ATCC 27774. *Biochem. Biophys. Res. Commun.* **2000**, *268*, 745−749.
(13) Andrade, S. L.; Brondino, C. D.; Feio, M. J.; Moura, I.; Moura, J. J. Aldehyde oxidoreductase activity in *Desulfovibrio alaskensis* NCIMB 13491 EPR assignment of the proximal [2Fe−2S] cluster to the Mo site. *Eur. J. Biochem.* **2000**, *267*, 2054−2061.
(14) Thapper, A.; Rivas, M. G.; Brondino, C. D.; Ollivier, B.; Fauque, G.; Moura, I.; Moura, J. J. Biochemical and spectroscopic characterization of an aldehyde oxidoreductase isolated from *Desulfovibrio aminophilus. J. Inorg. Biochem.* **2006**, *100*, 44−50.
(15) Romão, M. J.; Archer, M.; Moura, I.; Moura, J. J.; LeGall, J.; Engh, R.; Schneider, M.; Hof, P.; Huber, R. Crystal structure of the xanthine oxidase-related aldehyde oxido-reductase from *D. gigas*. *Science* **1995**, *270*, 1170−1176.
(16) Rebelo, J. M.; Dias, J. M.; Huber, R.; Moura, J. J.; Romão, M. J.; Structure refinement of the aldehyde oxidoreductase from *Desulfovibrio gigas* (MOP) at 1.28 Å. *J. Biol. Inorg. Chem.* **2001**, *6*, 791−800.
(17) Rebelo, J.; Macieira, S.; Dias, J. M.; Huber, R.; Ascenso, C. S.; Rusnak, F.; Moura, J. J.; Moura, I.; Romão, M. J. Gene sequence and crystal structure of the aldehyde oxidoreductase from *Desulfovibrio desulfuricans* ATCC 27774. *J. Mol. Biol.* **2000**, *297*, 135−146.
(18) Romão, M. J.; Cunha, C. A.; Brondino, C. D.; Moura, J. J. Molybdenum enzymes in reactions involving aldehydes and acids. *Met. Ions Biol. Syst.* **2002**, *39*, 539−570.
(19) Almendra, M. J.; Brondino, C. D.; Gavel, O.; Pereira, A. S.; Tavares, P.; Bursakov, S.; Duarte, R.; Caldeira, J.; Moura, J. J.; Moura, I. Purification and characterization of a tungsten-containing formate dehydrogenase from *Desulfovibrio gigas*. *Biochemistry* **1999**, *38*, 16366−16372.
(20) Brondino, C. D.; Passeggi, M. C.; Caldeira, J.; Almendra, M. J.; Feio, M. J.; Moura, J. J.; Moura, I. Incorporation of either molybdenum or tungsten into formate dehydrogenase from *Desulfovibrio alaskensis* NCIMB 13491; EPR assignment of the proximal iron−sulfur cluster to the pterin cofactor in formate dehydrogenases from sulfate-reducing bacteria. *J. Biol. Inorg. Chem.* **2004**, *9*, 145−151.
(21) Costa, C.; Teixeira, M.; LeGall, J.; Moura, J. J. G.; Moura, I. Formate dehydrogenase from *Desulfovibrio desulfuricans* ATCC 27774: Isolation and spectroscopic characterization of the active sites (heme, iron−sulfur centers and molybdenum). *J. Biol. Inorg. Chem.* **1997**, *2*, 198−208.
(22) Buc, J.; Santini, C. L.; Giordani, R.; Czjzek, M.; Wu, L. F.; Giordano, G. Enzymatic and physiological properties of the tungsten-substituted molybdenum TMAO reductase from *Escherichia coli*. *Mol. Microbiol.* **1999**, *32*, 159−168.
(23) Raaijmakers, H.; Teixeira, S.; Dias, J. M.; Almendra, M. J.; Brondino, C. D.; Moura, I.; Moura, J. J.; Romão, M. J. Tungsten-containing formate dehydrogenase from *Desulfovibrio gigas*: Metal identification and preliminary structural data by multiwavelength crystallography. *J. Biol. Inorg. Chem.* **2001**, *6*, 398−404.
(24) Raaijmakers, H.; Macieira, S.; Dias, J. M.; Teixeira, S.; Bursakov, S.; Huber, R.; Moura, J. J.; Moura, I.; Romão, M. J. Gene sequence and the 1.8 Å crystal structure of the tungsten-containing formate dehydrogenase from *Desulfovibrio gigas*. *Structure* **2002**, *10*, 1261−1272.
(25) Huber, R.; Hof, P.; Duarte, R. O.; Moura, J. J.; Moura, I.; Liu, M. Y.; LeGall, J.; Hille, R.; Archer, M.; Romão, M. J. A structure-based catalytic mechanism for the xanthine oxidase family of molybdenum enzymes. *Proc. Natl. Acad. Sci. U.S.A.* **1996**, *93*, 8846−8851.
(26) Bonin, I.; Martins, B. M.; Purvanov, V.; Fetzner, S.; Huber, R.; Dobbek, H. Active site geometry and substrate recognition of the molybdenum hydroxylase quinoline 2-oxidoreductase. *Structure* **2004**, *12*, 1425−1435.
(27) Okamoto, K.; Matsumoto, K.; Hille, R.; Eger, B. T.; Pai, E. F.; Nishino, T. The crystal structure of xanthine oxidoreductase during catalysis: Implications for reaction mechanism and enzyme inhibition. *Proc. Natl. Acad. Sci. U.S.A.* **2004**, *101*, 7931−7936.
(28) Hille, R.; Sprecher, H. On the mechanism of action of xanthine oxidase. Evidence in support of an oxo transfer mechanism in the molybdenum-containing hydroxylases. *J. Biol. Chem.* **1987**, *262*, 10914−10917.
(29) Boyington, J. C.; Gladyshev, V. N.; Khangulov, S. V.; Stadtman, T. C.; Sun, P. D. Crystal structure of formate dehydrogenase H: Catalysis involving Mo, molybdopterin, selenocysteine, and an $Fe_4S_4$ cluster. *Science* **1997**, *275*, 1305−1308.
(30) Jormakka, M.; Tornroth, S.; Byrne, B.; Iwata, S. Molecular basis of proton motive force generation: Structure of formate dehydrogenase-*N*. *Science* **2002**, *295*, 1863−1868.
(31) George, G. N.; Colangelo, C. M.; Dong, J.; Scott, R. A.; Khangulov, S. V.; Gladyshev, V. N.; Stadtman, T. C. X-ray absorption spectroscopy of molybdenum site of *Escherichia coli* formate dehydrogenase. *J. Am. Chem. Soc.* **1998**, *120*, 1267−1273.
(32) George, G. N. C.; Costa, C.; Moura, J. J. G.; Moura, I. Observation of ligand-based redox chemistry at the active site of a molybdenum enzyme. *J. Am. Chem. Soc.* **1999**, *121*, 2625−2626.
(33) Khangulov, S. V.; Gladyshev, V. N.; Dismukes, G. C.; Stadtman, T. C. Selenium-containing formate dehydrogenase H from *Escherichia coli*: A molybdopterin enzyme that catalyzes formate oxidation without oxygen transfer. *Biochemistry* **1998**, *37*, 3518−3528.

(34) Pleune, B.; Poli, R.; Fettinger, J. C. Synthesis and structure of the stable paramagnetic cyclopentadienyl polyhydride complexes $[Cp^*MH_3(dppe)]^+$ (M = Mo, W): Stronger M−H bonds upon oxidation. *J. Am. Chem. Soc.* **1998**, *120*, 3257−3258.
(35) Bencini, A.; Gatteschi, D. EPR of exchange coupled systems, Springer-Verlag: Berlin, Germany, 1990.
(36) Pilbrow, J. *Transition Ion Electron Paramagnetic Resonance*; Clarendon Press: Oxford, U.K., 1990.
(37) Caldeira, J.; Belle, V.; Asso, M.; Guigliarelli, B.; Moura, I.; Moura, J. J.; Bertrand, P. Analysis of the electron paramagnetic resonance properties of the $[2Fe-2S]^{1+}$ centers in molybdenum enzymes of the xanthine oxidase family: Assignment of signals I and II. *Biochemistry* **2000**, *39*, 2700−2707.
(38) Salikhov, K. M.; Galeev, R. T.; Voronkova, V. K.; Yablokov, Yu. V.; Legendziewicz, J. The reverse shift of the EPR line of paramagnetic centers coupled to species with a fast paramagnetic relaxation. *Appl. Magn. Reson.* **1998**, *14*, 457−472.
(39) Bertrand, P.; Roger, G.; Gayda, J. P. Measurement of the spin-lattice relaxation time from the broadening of the EPR spectrum of a randomly oriented system with $S = {}^1/_2$: Application to iron−sulfur proteins. *J. Magn. Reson.* **1980**, *40*, 539−549.
(40) Boer, D. R.; Thapper, A.; Brondino, C. D.; Romão, M. J.; Moura, J. J. G. X-ray crystal structure and EPR-spectra of "arsenite-inhibited" *Desulfovibrio gigas* aldehyde dehydrogenase; a member of the xanthine oxidase family. *J. Am. Chem. Soc.* **2004**, *126*, 8614−8615.
(41) Brondino, C. D.; Romão, M. J.; Moura, I.; Moura, J. J. G. Molybdenum and tungsten enzymes: The xanthine oxidase family. *Curr. Opin. Chem. Biol.* **2006**, *10*, 109−114.

AR050104K